Journal of Cleaner Production xxx (xxxx) xxx

Contents lists available at ScienceDirect

Journal of Cleaner Production

journal homepage: www.elsevier.com/locate/jclepro

Process simulation, optimization and assessment of post-combustion carbon dioxide capture with piperazine-activated blended absorbents

Bingtao Zhao [a, b, *], Tongbo Fang [a], Weifeng Qian [a], Jinpeng Liu [a], Yaxin Su [c]

[a] School of Energy and Power Engineering and Shanghai Key Laboratory of Multiphase Flow and Heat Transfer in Power Engineering, University of Shanghai for Science and Technology, 516 Jungong Road, Shanghai, 200093, China
[b] Key Laboratory of Low-grade Energy Utilization Technologies and Systems, Ministry of Education of China, Chongqing University, Chongqing, 400044, China
[c] School of Environmental Science and Engineering, Donghua University, 2999 North Renmin Road, Shanghai, 201620, China

ARTICLE INFO

Article history:
Received 17 June 2020
Received in revised form
21 September 2020
Accepted 30 September 2020
Available online xxx

Handling editor Cecilia Maria Villas Bôas de Almeida

Keywords:
Post-combustion CO_2 capture
Piperazine-activated blended absorbents
Process simulation
Multi-objective optimization

ABSTRACT

High efficiency, large capacity, and low energy consumption have become an important challenge in performances of post-combustion carbon dioxide (CO_2) capture and regeneration. Blended absorbents have shown great potential but their process simulation, modeling, and optimization have not been known definitively. This work developed the blended aqueous absorbents based on piperazine (PZ) activators: PZ-activated methyldiethanolamine (MDEA), potassium carbonate solution (K_2CO_3), and aqueous ammonia (NH_3H_2O) to improve their techno-economic performances. The whole process simulation was conducted using a validated rate-based model under given a CO_2 capture efficiency of 85%. In this process, the key factors including the molar concentration of the absorbent, PZ molar ratio, CO_2 load of lean liquid, lean-liquid temperature, flue-gas temperature, and rich-liquid temperature, were employed for the design of experiment using response surface methodology. A series of nonlinear regression equations were developed using the flow rate of absorbents, the reboiler heat duty (in the units of gigajoules per ton of CO_2), and the cooling-water flow rate as the multi-objective function. Subsequently, the optimal Pareto solution set and compromise solutions were determined using the multi-objective genetic algorithm and finally, their performances were assessed using the fuzzy close-degree algorithm. It was found that the optimal operating parameters can be determined effectively according to the proposed approach. For each PZ-activated blended absorbents, the trade-off effect exists between absorbent flow rate, reboiler heat duty, and cooling water consumption. The absorbents having optimal techno-economic performance were recommended to be PZ-activated MDEA, followed by PZ-activated K_2CO_3 and PZ-activated NH_3H_2O when considering the regeneration energy consumption. The results may provide a positive reference for process design and optimization of the industrial post-combustion CO_2 capture system.

1. Introduction

Post-combustion carbon dioxide (CO_2) capture is one of the effective ways to achieve CO_2 emission reductions from fossil fuel combustion and biomass incineration in power plants (Sun et al., 2020; Zhao et al., 2012). Compared with physicochemical adsorption (Ahmed et al., 2020), membrane separation (Hosseinzadeh et al., 2017), and direct air capture (Fasihi et al., 2019), chemical absorption is considered to be an advanced and mature technology, and has been widely used in the field of industrial carbon capture (Molina, 2015; Zarogiannis et al., 2016; Afkhamipour and Mofarahi, 2018).

Over the past decades, chemical absorption-based CO_2 capture has been extensively investigated via numerical simulations and experimental measurements. For instance, the various operating parameters were simulated to examine the effects on CO_2 capture efficiency, regeneration-energy consumption as well as exergy efficiency. The process optimization and the technical performances

* Corresponding author. School of Energy and Power Engineering and Shanghai Key Laboratory of Multiphase Flow and Heat Transfer in Power Engineering, University of Shanghai for Science and Technology, 516 Jungong Road, Shanghai, 200093, China.
E-mail addresses: zhaobingtao@usst.edu.cn, zhaobingtao@126.com (B. Zhao).

https://doi.org/10.1016/j.jclepro.2020.124502
0959-6526/

Nomenclature

a^I	Interfacial area (m^2)
a_p	specific area of the packing (m^2/m^3)
A_t	cross-sectional area of the column (m^2)
C_p	specific molar heat capacity (J/(kmol·K))
d_{eq}	equivalent diameter (m)
$D^L_{i,k}$	diffusivity of the liquid (m^2/s)
$D^V_{i,k}$	diffusivity of the vapor (m^2/s)
$\overline{D}$	average diffusivity (m^2/s)
g^{ex}	excess Gibbs energy (kJ/mol)
h	heat transfer coefficient ($W/(m^2·K)$)
h_p	height of the packed section (m)
i_L	residence time for the liquid (s)
$k^L_{i,k}$	mass transfer coefficient for the liquid (m/s)
$k^V_{i,k}$	mass transfer coefficient for the vapor (m/s)
$\overline{k}$	average mass transfer coefficient (m/s)
P	gas-phase pressure (kPa)
R	gas constant, R = 8.314 (J/(mol•K))
Re_v	Reynolds number for the vapor
$Sc_{V,i,k}$	Schmidt number for the vapor
T	temperature (K)
V_m	molar volume (m^3/mol)

Greek letters

λ	thermal conductivity (W/(m·K))
$\overline{\rho}$	molar density (kmol/m^3)

were also determined for the different absorbents (Mores et al., 2012; Damartzis et al., 2016). Furthermore, the investigations were dedicated to reducing the cost to improve process feasibility and economics of the decarbonization process (Dinca, 2016; Bui et al., 2016; Dubois and Thomas, 2018; Li and Yu, 2016; Jiang et al., 2017). However, post-combustion CO_2 capture with high

Table 1
Summary of CO_2 capture with blended absorbents.

Author	Absorbents	Operating conditions	Reactor	Performances and comments
Samanta and Bandyopadhyay (2011)	PZ−MDEA	Experiment: C_{MDEA} = 1.89−2.56 kmol/m^3, C_{PZ} = 0−0.95 kmol/m^3, P_{CO2} = 2−14 kPa and T = 25−40 °C	Wetted wall contactor	Specific absorption rate (10^6kmol/(m2·s)): 1.32−28.8, Enhancement factor: 10.9−262.2
Yu et al. (2016)	PZ−NH_3H_2O	Experiment & Simulation: Q_G = 19.15 L/min, Q_L = 2−4.4 L/h, C_{NH3} = 2.87%−8.76% (wt), C_{PZ} = 0−6.96% (wt), C_{CO2} = 10.04%, T_G = 24.6−25.4 °C, T_L = 10.2−24.8 °C, H = 1.0 m and D = 0.06 m	Packed column	5 wt% NH_3H_2O and 5 wt% PZ with a CO_2 loading of 0.2 molCO_2/molNH_3 can achieve a CO_2 removal efficiency comparable with 30 wt% MEA solution with a CO_2 loading of 0.2 molCO_2/molMEA
Oexmann et al. (2008)	PZ−K_2CO_3	Simulation: Q_G = 577 kg/s, C_{K2CO3} = 22.1−38.7% (wt), C_{PZ} = 0−13.8% (wt), C_{CO2} = 15.9% (vol), T_G = 62 °C and T_L = 40 °C	Packed column	Heat duty (GJ/t CO_2): 2.4 for PZ-K_2CO_3 and 3.3 for MEA, Power loss for solvent regeneration (kWh/kg CO_2): 0.288 for PZ-K_2CO_3 and 0.342 for MEA
Sun et al. (2005)	PZ−AMP	Simulation: C_{AMP} = 1.0−1.5 kmol/m^3, C_{PZ} = 0.1−0.4 kmol/m^3, T = 30−40 °C, H = 0.1 m and D = 0.0254 m	Wetted wall column	Absorption rate (10^8 kmol/s): 3.12−4.64
Li et al. (2013)	PZ−NH_3H_2O	Experiment: Q_G = 300 L/h, Q_L = 6−7.2 L/h, C_{NH3} = 0−4.12 mol/L, C_{PZ} = 0−0.5 mol/L, C_{CO2}:C_{NH3} = 0−0.5 (mol/mol), T = 10−15 °C, H = 0.1032 m and D = 0.0127 m	Bench-scale wetted-wall apparatus	Mass transfer coefficient (mmol/(s·kPa·m^2)): 0.3724−1.6899
Liu et al. (2012)	PZ−NH_3H_2O	Experiment & Simulation: Q_L = 3e6 m^3/s, C_{NH3} = 0.53−4 mol/L, C_{PZ} = 0.1−0.4 mol/L, $P_{CO2,i}$ = 8−25 kPa and T = 10−40 °C	Wetted wall column	Mass transfer coefficient (mmol/(s·kPa·m^2)): 0.56−1.289
Luo et al. (2005)	PZ/MEA/DEA−K_2CO_3	Experiment: Q_G = 41.6−124.9 kmol/(m^2·h), Q_L = 5.09−15.28 m^3/(m^2·h), C_{K2CO3} = 0.26−1.16 kmol/m^3, C_{PZ} = 0.005−0.02 kmol/m^3, C_{CO2} = 0.1−1.0% (vol), T = 25 ± 1 °C, H = 0.94 m and D = 0.05 m	Random packing column	PZ can improve the CO_2 absorption efficiency by 2−3 times that of MEA and DEA
Arshad et al. (2014)	PZ−K_2CO_3	Simulation: C_{K2CO3} = 20−40% (wt), C_{PZ} = 0.1−0.6 mol/kg and T_L = 25−120 °C	Flash column	The simulations match well with the source data
Liu et al. (2017)	AMP−MDEA	Experiment: C_{MDEA} = 20−30 wt%, C_{AMP} = 0−9 wt%, and T_L = 30−50 °C	Absorption bottle	AMP promotes the CO_2 absorption rate: from 5.7 to 7.3 × 10^8 kmol/s
Mudhasakul et al. (2013)	PZ−MDEA	Simulation: Q_G = 13203 kmol/h, Q_L = 32585 kmol/h, C_{MDEA} = 45% (wt), C_{PZ} = 5% (wt), C_{CO2} = 19.31% (mol), T_L = 52 °C, H = 14.1 m and D = 4.1 m	Packed column	The optimized PZ concentration found to be approximate 5 wt%
Zhao et al. (2017)	PZ−MDEA	Simulation: Q_G = 540 t CO_2/h, C_{MDEA} = 30−45 wt%, C_{PZ} = 5−20 wt%, C_{CO2}:$C_{MDEA,PZ}$ = 0.02−0.16, P_{abs} = 0.1−4.5 MPa, P_{strip} = 0.13−0.23 MPa, Absorber H = 18 m, D = 6 m, Stripper H = 1 m and D = 8 m	Packed column	The net power efficiency penalty of the PZ-MEA-based process is 7.66%, which is 16.1% less than that of the optimal MEA-based process (9.13%)

Note.

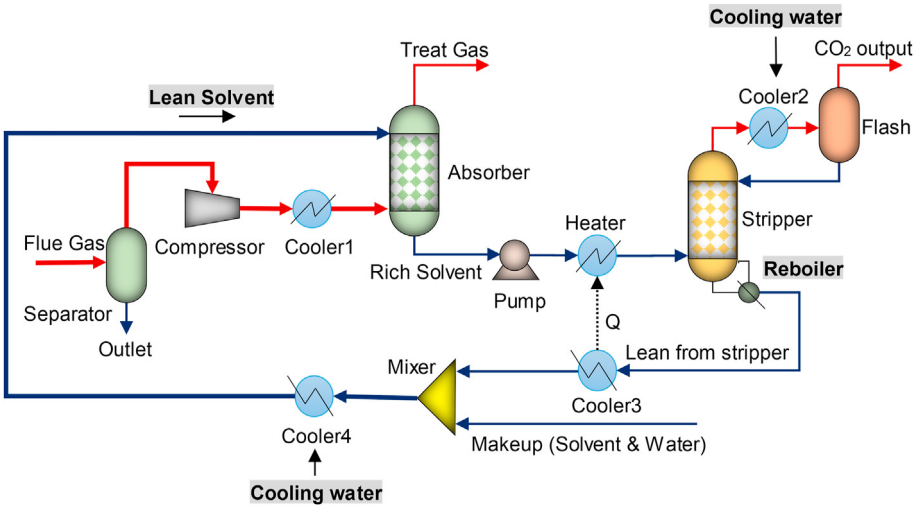

Fig. 1. Schematic diagram of the post-combustion CO_2 capture process.

Table 2
The operating parameters (Zhou, 2008).

Parameters	Specification	Value
Post-combustion CO_2	Coal-fired power plant	430 MW (generation capacity)
Flue Gas	Flow rate (kmol/h)	69738.9
	Pressure (bar)	1.0
	Input temperature (°C)	57.8
	Composition	12.8% CO_2, 2.9% O_2, 68.3%N_2 and 16% H_2O
Absorber/Stripper	Pressure (bar)	1.2
	Packing	MELLAPAK (Model: 250Y)
	Height of the equal plate (m)	0.5
	Number of trays (N)	10

efficiency, large capacity, and low regenerative energy consumption still faces a great challenge in its techno-economic performances.

To date, the large-scale applications of conventional single absorbents for CO_2 capture are often limited because of its high regenerative energy consumption, easy degradability, and low absorption rates. State-of-the-art studies have demonstrated that these inherent disadvantages can be overcome with the blended absorbents. Comparisons have also indicated that the blended absorbent is superior to the individual absorbent including monoethanolamine (MEA), methyldiethanolamine (MDEA), aqueous ammonia (NH_3H_2O) and piperazine (PZ) in decarburization performances (Yeh et al., 2005; Kemper et al., 2011; Dubois and Thomas, 2012; Gao et al., 2017). Furthermore, it is suggested that blended absorbents with amines including MEA, PZ, DEA (diethanolamine), and AMP (2-amino-2-methyl-1-propanol) as activators are beneficial for improving the technical performance (such as mass transfer rate and absorption capacity) and economic performance (benefit-cost ratio). The applications of the blended absorbents under different operating conditions and reactors for flue-gas decarburization, are summarized in Table 1.

Nevertheless, questions remain relating to post-combustion CO_2 capture with activated blended absorbents: Most of the previous work is only applicable to the lab/bench-scale experiments and simulations (accounting for approximately 1/2 and 2/3 of the total number investigations according to Table 1), the characterizations for industrial application are rare in particular for CO_2 capture with activated blended absorbents. Moreover, the multiple performance responses to the factors in particular the molar ratio of the activated agents are not reported for CO_2 capture with blended absorbents, even though the differences in the performance of individual absorbent (e.g., alkaline, amine, and ammonia) for CO_2 capture have been compared. That is, the contribution of activators in CO_2 capture performances and their specific role in the system have remained unknown. Finally, from the global process perspective, there are still gaps in the quantitative modeling and optimization of

Table 3
The Rate-based model.

Item for	Formula	Eq.	Ref.
Redlich-Kwong equation of state	$p = RT/(V_m - b) - a/\sqrt{T}V_m(V_m + b)$	(1)	Huamán (2017)
Electrolyte-NRTL method	$g^{ex}/RT = g^{ex,pdh}/RT + g^{ex,Born}/RT + g^{ex,lc}/RT + g^{ex,BG}/RT$	(2)	Huamán (2017)
Liquid binary mass transfer coefficient	$k^L_{i,k} = 2\sqrt{D^L_{i,k}/\pi i_L}$	(3)	Bravo et al. (1985)
Gas binary mass transfer coefficient	$k^V_{i,k} = 0.338D^V_{i,k}/d_{eq}Re^{0.8}_V Sc^{0.333}_{V,i,k}$	(4)	Bravo et al. (1985)
Interfacial area	$a^I = a_p A_t h_p$	(5)	Bravo et al. (1985)
Heat transfer coefficient	$h = \overline{k}\overline{\rho}C_p(\lambda/\overline{\rho}C_p\overline{D})^{2/3}$	(6)	Chilton and Colburn (1934)

Table 4
The phase equilibrium reaction and kinetic reaction equation.

Activated blended absorbents	Process	Reactions	Ref.
MEA[a]	Equilibrium	$2H_2O \leftrightarrow H_3O^+ + OH^-$	Arshad et al. (2014); Zhao et al. (2017); Yu et al. (2014); Bishnoi and Rochelle (2000); Li et al. (2016)
		$HCO_3^- + H_2O \leftrightarrow H_3O^+ + CO_3^{-2}$	Arshad et al. (2014); Zhao et al. (2017); Yu et al. (2014); Bishnoi and Rochelle (2000); Li et al. (2016)
		$MEA^+ + H_2O \leftrightarrow H_3O^+ + MEA$	Li et al. (2016)
		$MEACOO^- + H_2O \leftrightarrow HCO_3^- + MEA$	Li et al. (2016)
	Kinetics	$CO_2 + OH^- \rightarrow HCO_3^-$	Yu et al. (2014); Bishnoi and Rochelle (2000)
		$HCO_3^- \rightarrow CO_2 + OH^-$	Yu et al. (2014); Bishnoi and Rochelle (2000)
		$MEA + CO_2 + H_2O \rightarrow MEACOO^- + H_3O^+$	Li et al. (2016)
		$MEACOO^- + H_3O^+ \rightarrow MEA + CO_2 + H_2O$	Li et al. (2016)
PZ-K_2CO_3	Equilibrium	$2H_2O \leftrightarrow H_3O^+ + OH^-$	Arshad et al. (2014); Zhao et al. (2017); Yu et al. (2014); Bishnoi and Rochelle (2000); Li et al. (2016)
		$HCO_3^- + H_2O \leftrightarrow H_3O^+ + CO_3^{-2}$	Arshad et al. (2014); Zhao et al. (2017); Yu et al. (2014); Bishnoi and Rochelle (2000); Li et al. (2016)
		$PZH^+ + H_2O \leftrightarrow PZ + H_3O^+$	Arshad et al. (2014); Zhao et al. (2017); Yu et al. (2014); Bishnoi and Rochelle (2000)
		$HPZCOO + H_2O \leftrightarrow PZCOO^- + H_3O^+$	Arshad et al. (2014); Zhao et al. (2017); Yu et al. (2014); Bishnoi and Rochelle (2000)
	Kinetics	$CO_2 + OH^- \rightarrow HCO_3^-$	Yu et al. (2014); Bishnoi and Rochelle (2000)
		$HCO_3^- \rightarrow CO_2 + OH^-$	Yu et al. (2014); Bishnoi and Rochelle (2000)
		$PZ + CO_2 + H_2O \rightarrow PZCOO^- + H_3O^+$	Arshad et al. (2014); Zhao et al. (2017); Yu et al. (2014); Bishnoi and Rochelle (2000)
		$PZCOO^- + H_3O^+ \rightarrow PZ + CO_2 + H_2O$	Arshad et al. (2014); Zhao et al. (2017); Yu et al. (2014); Bishnoi and Rochelle (2000)
		$PZCOO^- + CO_2 + H_2O \rightarrow PZCOO^{-2} + H_3O^+$	Arshad et al. (2014); Zhao et al. (2017); Yu et al. (2014); Bishnoi and Rochelle (2000)
		$PZCOO^{-2} + H_3O^+ \rightarrow PZCOO^- + CO_2 + H_2O$	Arshad et al. (2014); Zhao et al. (2017); Yu et al. (2014); Bishnoi and Rochelle (2000)
PZ-MDEA	Equilibrium	$2H_2O \leftrightarrow H_3O^+ + OH^-$	Arshad et al. (2014); Zhao et al. (2017); Yu et al. (2014); Bishnoi and Rochelle (2000); Li et al. (2016)
		$HCO_3^- + H_2O \leftrightarrow H_3O^+ + CO_3^{-2}$	Arshad et al. (2014); Zhao et al. (2017); Yu et al. (2014); Bishnoi and Rochelle (2000); Li et al. (2016)
		$PZH^+ + H_2O \leftrightarrow PZ + H_3O^+$	Arshad et al. (2014); Zhao et al. (2017); Yu et al. (2014); Bishnoi and Rochelle (2000)
		$HPZCOO + H_2O \leftrightarrow PZCOO^- + H_3O^+$	Arshad et al. (2014); Zhao et al. (2017); Yu et al. (2014); Bishnoi and Rochelle (2000)
		$MDEAH^+ + H_2O \leftrightarrow MDEA + H_3O^+$	Zhao et al. (2017)
	Kinetics	$CO_2 + OH^- \rightarrow HCO_3^-$	Yu et al. (2014); Bishnoi and Rochelle (2000)
		$HCO_3^- \rightarrow CO_2 + OH^-$	Yu et al. (2014); Bishnoi and Rochelle (2000)
		$PZ + CO_2 + H_2O \rightarrow PZCOO^- + H_3O^+$	Arshad et al. (2014); Zhao et al. (2017); Yu et al. (2014); Bishnoi and Rochelle (2000)
		$PZCOO^- + H_3O^+ \rightarrow PZ + CO_2 + H_2O$	Arshad et al. (2014); Zhao et al. (2017); Yu et al. (2014); Bishnoi and Rochelle (2000)
		$PZCOO^- + CO_2 + H_2O \rightarrow PZCOO^{-2} + H_3O^+$	Arshad et al. (2014); Zhao et al. (2017); Yu et al. (2014); Bishnoi and Rochelle (2000)
		$PZCOO^{-2} + H_3O^+ \rightarrow PZCOO^- + CO_2 + H_2O$	Arshad et al. (2014); Zhao et al. (2017); Yu et al. (2014); Bishnoi and Rochelle (2000)
		$MDEA + CO_2 + H_2O \rightarrow MDEAH^+ + HCO_3^-$	Zhao et al. (2017)
		$MDEAH^+ + HCO_3^- \rightarrow MDEA + CO_2 + H_2O$	Zhao et al. (2017)
PZ-NH_3	Equilibrium	$2H_2O \leftrightarrow H_3O^+ + OH^-$	Arshad et al. (2014); Zhao et al. (2017); Yu et al. (2014); Bishnoi and Rochelle (2000); Li et al. (2016)
		$HCO_3^- + H_2O \leftrightarrow H_3O^+ + CO_3^{-2}$	Arshad et al. (2014); Zhao et al. (2017); Yu et al. (2014); Bishnoi and Rochelle (2000); Li et al. (2016)
		$PZH^+ + H_2O \leftrightarrow PZ + H_3O^+$	Arshad et al. (2014); Zhao et al. (2017); Yu et al. (2014); Bishnoi and Rochelle (2000)
		$HPZCOO + H_2O \leftrightarrow PZCOO^- + H_3O^+$	Arshad et al. (2014); Zhao et al. (2017); Yu et al. (2014); Bishnoi and Rochelle (2000)
		$NH_3 + H_2O \leftrightarrow NH_4^+ + OH^-$	Yu et al. (2014); Bishnoi and Rochelle (2000)
	Kinetics	$CO_2 + OH^- \rightarrow HCO_3^-$	Yu et al. (2014); Bishnoi and Rochelle (2000)
		$HCO_3^- \rightarrow CO_2 + OH^-$	Yu et al. (2014); Bishnoi and Rochelle (2000)
		$PZ + CO_2 + H_2O \rightarrow PZCOO^- + H_3O^+$	Arshad et al. (2014); Zhao et al. (2017); Yu et al. (2014); Bishnoi and Rochelle (2000)
		$PZCOO^- + H_3O^+ \rightarrow PZ + CO_2 + H_2O$	Arshad et al. (2014); Zhao et al. (2017); Yu et al. (2014); Bishnoi and Rochelle (2000)
		$PZCOO^- + CO_2 + H_2O \rightarrow PZCOO^{-2} + H_3O^+$	Arshad et al. (2014); Zhao et al. (2017); Yu et al. (2014); Bishnoi and Rochelle (2000)
		$PZCOO^{-2} + H_3O^+ \rightarrow PZCOO^- + CO_2 + H_2O$	Arshad et al. (2014); Zhao et al. (2017); Yu et al. (2014); Bishnoi and Rochelle (2000)
		$NH_3 + CO_2 + H_2O \rightarrow NH_2COO^- + H_3O^+$	Yu et al. (2014); Bishnoi and Rochelle (2000)
		$NH_2COO^- + H_3O^+ \rightarrow NH_3 + CO_2 + H_2O$	Yu et al. (2014); Bishnoi and Rochelle (2000)
		$NH_4HCO_3 \leftrightarrow NH_4^+ + HCO_3^-$	Yu et al. (2014); Bishnoi and Rochelle (2000)

Note: [a] for model validation.

the entire decarburization and regeneration, when considering the interaction of multi-factors on the techno-economic parameters.

To overcome the aforementioned problems, this work proposes a combined approach to simulate, optimize, and assess the entire absorption-desorption process of post-combustion CO_2 capture with the optimized activated blended absorbents from a commercial power plant. First, the process simulation was developed and validated based on the key factors and objective variables. Subsequently, the nonlinear regression equation was obtained based on the response surface methodology and, the comprehensive assessment of CO_2 capture performance was implemented using multi-objective optimization based on genetic algorithm. Their respective optimal blending schemes were finalized and compared to guide the industrial applications.

Absorbents: PZ = piperazine, MEA = monoethanolamine, MDEA = methyldiethanolamine, NH_3H_2O = aqueous ammonia, AMP = 2-amino-2-methyl-1-propanol.

Operating parameters and reactor dimensions: Q = flow rate (m^3/s), C = concentration (vol%, wt.% or kmol/m^3), T = temperature (^oC), P = pressure (Pa), D = reactor diameter (m), H = reactor height (m).

2. Process flow and methods

2.1. Post-combustion CO_2 capture system

Fig. 1 shows the process flow of CO_2 capture from exhaust flue gas of a typical coal-fired power plant. In the industrial installation, it is necessary to include both CO2 capture and absorbent regeneration unit, while the packed column is a high-efficiency and technologically mature device. Hence, the system actually can be divided into an absorption unit (absorber) and a desorption unit (stripper). Standard packing (Model: MELLAPAK-250Y, SULZER Ltd) was used in both units, with 10 stage numbers and 0.5m intervals. The entire process was operated in a closed-cycle mode, and the original operating parameters are shown in Table 2.

PZ-activated methyldiethanolamine (MDEA), potassium carbonate solution (K_2CO_3), and aqueous ammonia (NH_3H_2O) were chosen as the blended absorbents, because the primary absorbents K_2CO_3, MDEA, and NH_3H_2O are widely-used industrial typical absorbents, representing the carbonates, amines, and ammonia respectively. Particularly, PZ was used as the activator because of its superior

Table 5
Design of experiment using response surface methodology.

No.	PZ molar concentration ratio (%)	Lean solvent CO_2 loading (molCO_2/molAbsorbent)	Total molar concentration of absorbent (mol·L^{-1})	Lean solvent temperature (^oC)	Rich solvent temperature (^oC)
	x_1	x_2	x_3	x_4	x_5
1	20	0.2	3	30	90
2	40	0.2	4	40	90
3	40	0.2	3	40	85
4	30	0.2	3	40	90
5	30	0.2	4	40	85
6	30	0.25	3	30	90
7	40	0.15	3	40	90
8	20	0.2	3	40	85
9	20	0.15	3	40	90
10	30	0.2	3	30	95
11	30	0.2	3	40	90
12	30	0.25	3	40	95
13	30	0.2	3	40	90
14	30	0.2	2	40	85
15	30	0.15	3	40	85
16	30	0.2	4	50	90
17	20	0.2	2	40	90
18	30	0.2	3	50	95
19	30	0.2	3	30	85
20	30	0.15	2	40	90
21	30	0.25	2	40	90
22	30	0.2	3	40	90
23	30	0.25	4	40	90
24	30	0.2	2	40	95
25	30	0.2	4	40	95
26	40	0.2	3	50	90
27	20	0.2	3	40	95
28	40	0.2	2	40	90
29	30	0.2	2	50	90
30	20	0.2	4	40	90
31	30	0.2	3	40	90
32	30	0.2	2	30	90
33	30	0.2	3	50	85
34	20	0.2	3	50	90
35	30	0.15	3	40	95
36	30	0.25	3	50	90
37	40	0.2	3	40	95
38	30	0.15	3	30	90
39	40	0.2	3	30	90
40	30	0.15	4	40	90
41	30	0.25	3	40	85
42	30	0.15	3	50	90
43	40	0.25	3	40	90
44	20	0.25	3	40	90
45	30	0.2	3	40	90
46	30	0.2	4	30	90

activation ability compared to MEA and DEA (Luo et al., 2005).

2.2. Methods

2.2.1. Reaction mechanisms

The Rate-based model (Zhang and Guo, 2013a,b) was used to simulate mass transfer and reaction in the decarburization process. This model comprehensively covers the properties of the gas and liquid phases, mass/heat transfer coefficients, as well as interface area (Huamán, 2017; Bravo et al., 1985; Chilton and Colburn, 1934), as shown in Table 3. To characterize the physicochemical performances of CO_2 capture more accurately, both phase equilibrium and kinetic reactions were considered throughout the process (Yu et al., 2014; Bishnoi and Rochelle, 2000; Li et al., 2016), as listed in Table 4. Note that this process is based on the following assumptions: ignoring the effects of SO_2 and NO_x; ignoring the reaction of O_2 with the absorbents; not considering the corrosion and degradation of the absorbents.

2.3. Influencing factors and multi-objective performance parameters

During the entire absorption and desorption process of CO_2 capture, the CO_2 load of lean solvent, total molar concentration of absorbent, lean solvent temperature, and rich-liquid temperature are generally considered to be important factors under specified flue gas parameters (Yu et al., 2016; Oexmann et al., 2008). Besides, it is necessary to include the PZ molar ratio as a key factor in this work due to the utilization of the activated-solution strategy. All these five factors were chosen as decision variables to address the impact on the critical techno-economic indicators (objective variables) under specified CO_2 capture efficiency. The latter refers to the absorbent circulation flow rate, reboiler heat duty (in the units of gigajoules per ton of CO_2), and cooling water consumption (including those for the stripper and lean liquid).

2.3.1. Design, modeling and optimization

Based on the significance test of the single factor, the response surface methodology was used for global experimental design to obtain the combined effects of multiple factors. In this process, the Box-Behnken design was used as shown in Table 5. Based on the simulation results of full-process CO_2 capture and regeneration, the multi-objective response surface equations were established using multiple regression analysis. Subsequently, the optimal Pareto solution set is obtained using the multi-objective genetic algorithm. According to the principle of fuzzy close-degree, the optimal compromise solution was finally determined for further assessment.

3. Results and discussion

3.1. Model validation

To verify the accuracy and reliability of the process simulations, a comparative inspection process is necessary prior to performing the present work. Note that in this process, the models and methods developed in this work were employed but the operating parameters reported in the comparative literatures were used, respectively.

Figs. 2–4 show the comparisons between the present simulation and the source data reported by refs. (Chapel et al., 1999; Sakwattanapong et al., 2005; Wilson et al., 2004; Zhou, 2008; Alie et al., 2005). Although not all the source data used are experimental, the data simulated by ASPEN Plus is usually considered credible. According to the error analysis, the present simulation in the objective techno-economic indicators was found to match the source values with the mean relative error (MRE) of 3.343%–14.876% for the cases. Because of the complexity and cost of modeling and computational processes, the agreement is considered to be acceptable. It is suggested that the proposed approach is feasible for the further process simulation of the post-combustion CO_2 capture.

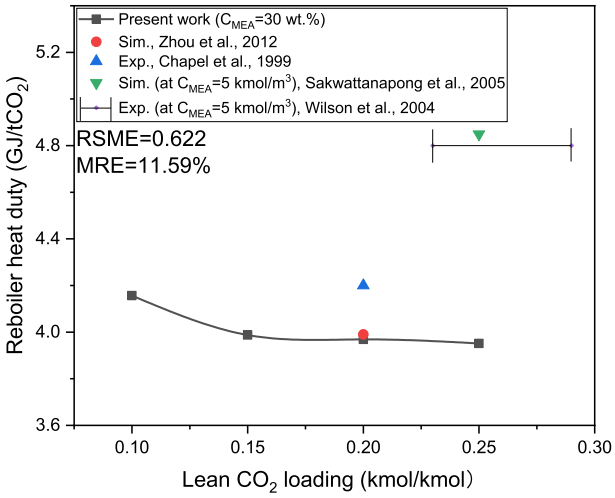

Fig. 2. Comparison of the present simulation with results by Zhou (2008) for reboiler heat duty.

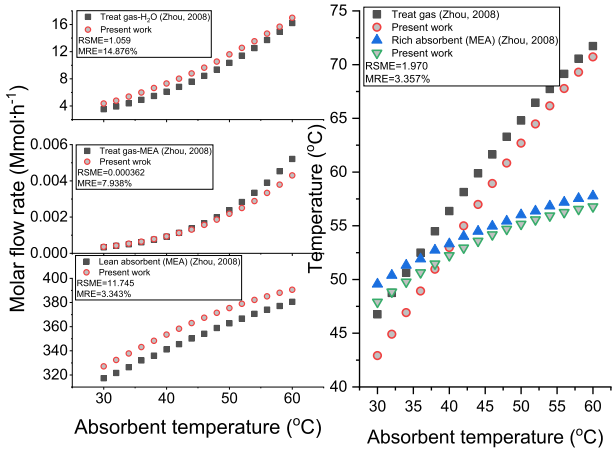

Fig. 3. Comparison of the present simulation with results by Zhou (2008) for flow rate and temperature of absorber and stripper.

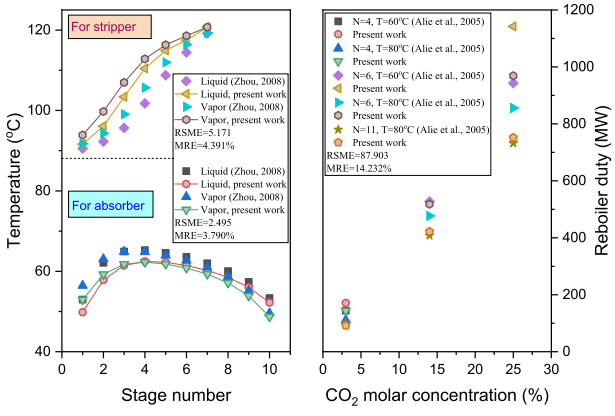

Fig. 4. Comparison of the present simulation with results by Zhou (2008) and Alie et al. (2005).

Table 6
Regression equations for piperazine-activated blended absorbents.

Item	Coef.	PZ activated K_2CO_3 blended absorbent			PZ activated MDEA blended absorbent			PZ activated NH_3H_2O blended absorbent		
		R_1	R_2	R_3	R_1	R_2	R_3	R_1	R_2	R_3
c	a_0	40295.717	69.633	661.272	318.225	64.919	443.835	4211.095	24.927	315.682
x_1	b_1	−145.996	−0.556	−4.780	16.606	0.108	−1.433	10.158	−0.068	−1.494
x_2	b_2	−1243.617	−10.745	66.717	−5199.887	−99.634	−763.476	−7164.718	30.594	286.760
x_3	b_3	−3076.892	−11.191	−115.244	−201.041	−1.917	−23.165	−984.230	−5.606	−54.052
x_4	b_4	−80.461	−0.219	−7.314	−28.957	0.544	−1.171	−50.371	0.113	−5.642
x_5	b_5	−667.444	−0.664	−4.303	38.366	−1.270	−4.644	9.085	−0.238	−0.731
x_1x_2	b_{12}	17.735	0.730	6.109	−47.014	0.326	3.925	−85.527	0.043	4.060
x_1x_3	b_{13}	16.530	0.081	0.599	0.612	0.016	0.146	4.357	3.488exp(-3)	0.022
x_1x_4	b_{14}	0.890	1.897exp(-3)	0.021	−0.624	1.447exp(-3)	1.400exp(-3)	−0.730	−8.000exp(-4)	4.840exp(-3)
x_1x_5	b_{15}	−1.230exp(-4)	−1.211exp(-3)	−7.996exp(-3)	1.568exp(-5)	−1.533exp(-3)	0.018	3.379exp(-4)	8.630exp(-4)	6.466exp(-3)
x_2x_3	b_{23}	−1530.733	5.831	50.458	−626.124	−1.681	−10.062	−2272.278	−3.177	−25.520
x_2x_4	b_{24}	−364.489	−0.466	−12.094	218.862	0.020	2.044	330.819	0.512	0.675
x_2x_5	b_{25}	−0.0534	−1.260	−7.182	−1.699exp(-3)	1.009	7.053	2.724exp(-12)	−0.493	−3.069
x_3x_4	b_{34}	23.121	0.047	0.932	−11.251	−0.014	0.067	−9.015	−0.018	0.245
x_3x_5	b_{35}	−3.514exp(-3)	0.011	0.056	1.174 exp(-3)	0.016	0.119	−8.231exp(-14)	0.043	0.217
x_4x_5	b_{45}	−9.600exp(-4)	3.126exp(-4)	4.442exp(-3)	−8.273exp(-4)	−6.887exp(-3)	−0.027	1.504exp(-14)	−2.083exp(-3)	−6.344exp(-3)
$(x_1)^2$	b_{11}	0.660	2.803exp(-3)	0.021	0.094	−1.490exp(-3)	−0.019	0.029	−2.321exp(-4)	−7.399exp(-3)
$(x_2)^2$	b_{22}	81368.659	275.038	2134.809	6799.520	−9.698	−174.334	27026.968	23.419	60.840
$(x_3)^2$	b_{33}	234.114	0.621	5.339	67.269	0.087	0.448	182.139	0.329	3.212
$(x_4)^2$	b_{44}	0.524	7.280exp(-4)	0.055	0.860	1.650exp(-3)	0.032	0.848	1.342exp(-3)	0.050
$(x_5)^2$	b_{55}	3.708	4.658exp(-3)	0.030	−0.213	6.748exp(-3)	0.014	−0.051	9.156exp(-4)	2.065exp(-3)
Statistics	Mean Square	6.733exp(5)	1.780	427.14	2.122exp(5)	1.090	66.300	5.395exp(5)	1.61	248.09
	F	22.125	16.150	41.84	368.970	34.45	20.190	572.350	702.050	103.75
	P	<0.0001	<0.0001	<0.0001	<0.0001	<0.0001	<0.0001	<0.0001	<0.0001	<0..0001
	Std.Dev.	174.443	0.332	3.210	23.980	0.180	1.810	30.70	0.048	1.55
	Mean	1802.960	4.760	38.130	1183.540	2.620	24.120	1949.41	0.048	47.940
	C.V.%	9.680	6.970	8.410	2.030	6.790	7.510	1.570	0.818	3.230
	R^2	0.947	0.928	0.971	0.997	0.966	0.944	0.998	0.998	0.988
	Adj-R^2	0.904	0.871	0.947	0.994	0.938	0.897	0.996	0.997	0.979
	Pred-R^2	0.786	0.713	0.883	0.986	0.857	0.759	0.991	0.993	0.952
	Adeq Prec	20.207	16.458	27.289	81.233	25.172	19.525	91.641	101.423	43.439

Remark:
$\times\ _2{+}b_{13}\times 1\times\ _3{+}b_{14}\times 1\times\ _4{+}b_{15}\times 1\times\ _5{+}b_{23}\times 2\times\ _3{+}b_{24}\times 2\times\ _4{+}b_{25}\times 2\times\ _5{+}b_{34}\times 3\times\ _4{+}b_{35}\times 3\times\ _5{+}b_{45}\times 4\times\ _5{+}b_{11}\times\ ^2_1{+}b_{22}\times\ ^2_2{+}b_{33}\times\ ^2_3{+}b_{44}\times\ ^2_4{+}b_{55}\times\ ^2_5$.
c: Constant; x_1: PZ molar concentration ratio (%); x_2: Lean solvent CO_2 loading ($molCO_2$/mol absorbent); x_3: Total molar concentration of absorbent ($mol{\cdot}L^{-1}$); x_4: Lean solvent temperature (°C); x_5: Rich solvent temperature (°C); R_1: Absorbent molar flow rate ($kmol/tCO_2$); R_2: Reboiler duty (GJ/tCO_2); R_3: Cooling water consumption (t/tCO_2).

3.2. Multi-objective regression and response

The simulation was performed (constrained to 85% CO_2 capture efficiency) according to the design scheme (Table 5). Usually, the capture efficiency of post-combustion CO_2 is set as approximately 75%–90%, e.g., 92.7% (Chen et al., 2016), 75% (Che et al., 2014), and 80% (Zhang et al., 2013), etc. It highly depends upon the trade-off strategy based on energy consumption per unit CO_2 (including both power consumption and heat consumption). 85% CO_2 capture efficiency is relatively acceptable according to Zhou et al. (2012). Hence, it was also used in this work, as reported by Alie et al. (2005). Multiple regression analyses were then carried out to obtain the corresponding coefficients and the statistical indexes for the response surface equations, as shown in Table 6. It is found to have $P < 0.0001$ and R^2 ranging 0.871–0.997 for all regression equations, indicating that the results are reliable and can be acceptable.

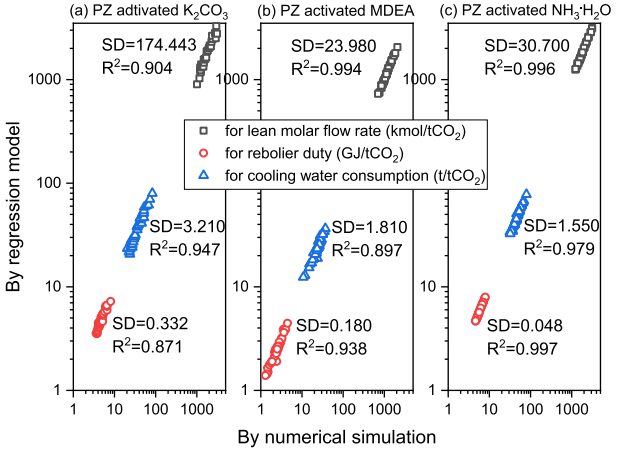

Fig. 5. Comparison of results between the numerical simulations and regression models based on the proposed response surface methodology: (a) PZ activated K_2CO_3, (b) PZ activated MDEA, and (c) PZ activated NH_3H_2O.

Fig. 5 illustrates the comparison between the numerical simulations and regression models based on the proposed response surface methodology. They are observed to match well. Furthermore, Fig. 6 presents the response of each objective variable to the decisive variables. It is found that the response of the objective variables to each decision variable is complex, and does not always present a monotonic relationship. For each techno-economic indicator, the influence relationship of each operating factor is not consistent due to the different interactions with other factors. It implies that their specific roles are variable when using different types of primary absorbents. In particular, the effect of the molar ratio is important for the activated blended absorbents. However, the high PZ molar ratio does not necessarily correspond to optimal operating conditions, because the CO_2 absorption and desorption depend on overall physicochemical processes.

3.3. Global optimization

A multi-objective optimization was further performed using the multi-objective genetic algorithm. In this process, the population size, the probability of hybridization, and the probability of evolutionary algebra were set to 100, 0.80, and 500, respectively.

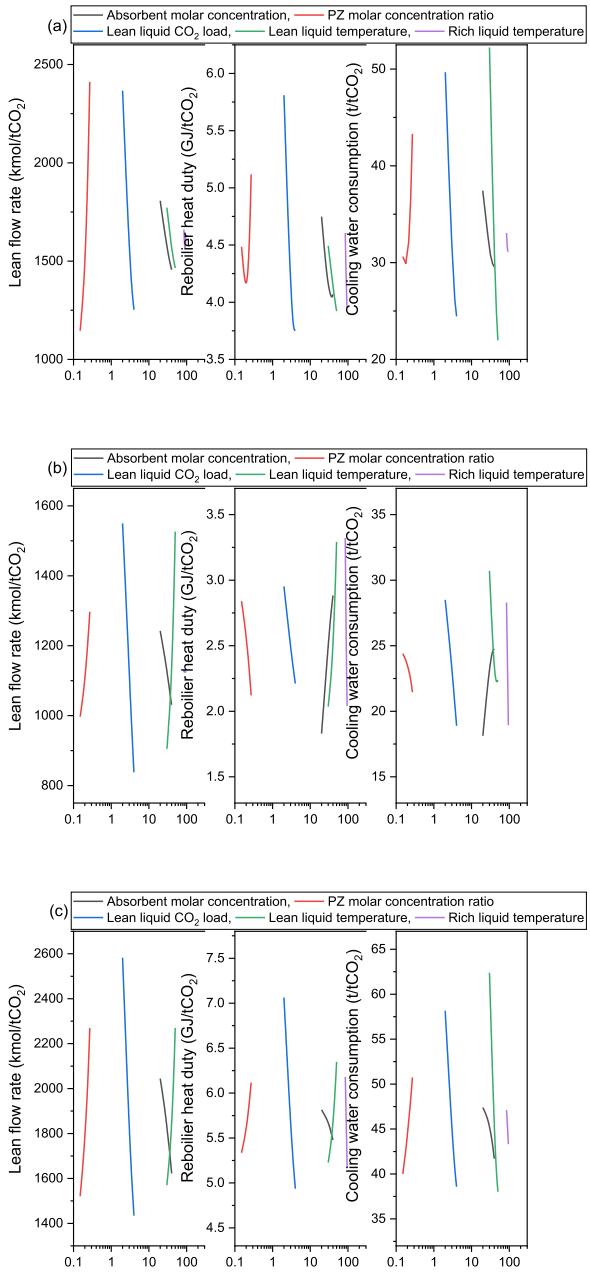

Fig. 6. Response of each objective variable to the decisive variables: (a) PZ activated K_2CO_3, (b) PZ activated MDEA, and (c) PZ activated NH_3H_2O.

Considering the randomicity of heuristic search, it was implemented 5 times repeatedly. A series of optimal Pareto solution sets are obtained for each blended absorbent, as shown in Fig. 7.

Usually, an optimal compromise solution is necessary for multi-objective problems in practice. In this work, we used the fuzzy close-degree algorithm to determine the optimal compromise solution. This algorithm computes fuzzy membership degree using a Gaussian membership function $\mu(f_{ij}) = \exp\{-[(f_{ij} - f^*)/1/m\sum_{j=1}^{m}|f_{ij} - f^*|)]^2\}$ (Sugeno, 1985) and using the fuzzy Hamming distance (Izadikhah, 2009) as the index of compromise (IOC) for comprehensive evaluation which can be expressed by $I(F_j, F^*) = 1 - 1/n\sum_{j=1}^{n}|w_j(1 - \mu(f_{ij}))|$,

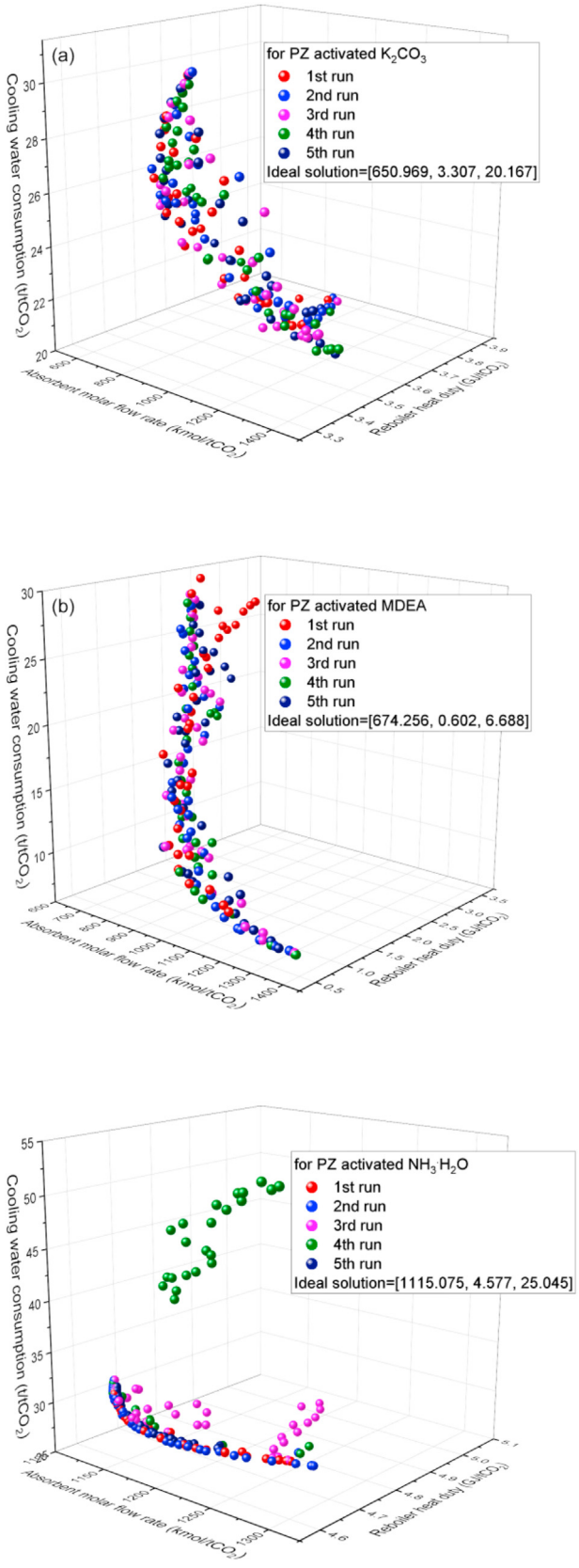

Fig. 7. Pareto solution set for (a) PZ activated K_2CO_3, (b) PZ activated MDEA, and (c) PZ activated NH_3H_2O.

Table 7
Optimal compromise solution for the PZ activated blended absorbents using fuzzy close-degree algorithm.

PZ activated blended absorbents	PZ molar concentration ratio (%)	Lean solvent CO_2 loading ($molCO_2$/mol absorbent)	Total molar concentration of absorbent ($mol{\cdot}L^{-1}$)	Lean solvent temperature (°C)	Rich solvent temperature (°C)	Lean molar flow rate (kmol/tCO_2)	Reboiler heat duty (GJ/tCO_2)	Cooling water consumption (t/tCO_2)
PZ-K_2CO_3	29.652	0.159	3.999	30.138	90.562	767.910	3.377	27.020
PZ-MDEA	20.153	0.249	3.992	34.509	92.328	925.668	0.617	11.925
PZ-NH_3H_2O	39.994	0.150	3.988	42.304	94.958	1125.856	4.653	27.967

where, F_j is one of the Pareto optimal solutions for objective functions: absorbent circulation flow rate, reboiler heat duty and cooling water consumptions, respectively. w is their weight here. It was determined by the analytic hierarchy process (AHP) by an evaluation matrix A = [1, 1/2, 2; 2, 1, 3; 1/2, 1/3, 1]. Then the weight vector was obtained as w = [0.30, 0.54, 0.16] with consistency ratio RI = 0.0079 < 0.1. F^* is the ideal solution in the Pareto optimal solution set. They were found to be [650.969, 3.307, 20.167] for PZ-activated K_2CO_3, [674.256, 0.602, 6.688] for PZ-activated MDEA and [1115.075, 4.577, 25.045] for PZ-activated NH_3H_2O, respectively. In terms of IOC, the Pareto solution corresponding to the minimum IOC is considered to be the optimal compromise solution, the final optimized results for the operating parameters are shown in Table 7.

3.4. Comparison and assessment

According to Table 7, the absorbent flow rate of PZ activated K_2CO_3 is found to be the lowest, followed by PZ activated MDEA and PZ activated NH_3H_2O. For the reboiler heat duty, the PZ activated MDEA is significantly less than the other two. A similar trend occurs in cooling water consumption. It is suggested that these technical-economic indicators have a trade-off effect. However, their minimum IOC seems to be similar, with 0.7574, 0.7574, and 0.7478, respectively.

Among the three indicators, the reboiler heat duty is usually considered to be a relatively important economic indicator under a given capture efficiency, as it involves most of the process energy consumption of post-combustion CO_2 capture (Zhou et al., 2012). The optimal compromise solution of reboiler heat duty for PZ activated K_2CO_3 was found to be 3.377 GJ/tCO_2. It is at a superior level (close to the lower limit) compared to the result reported by Oexmann et al. (2009), who presented a range from 3.63 GJ/tCO_2 for $K_{3.2}P_{1.6}$ (K_2CO_3:PZ = 28:8.7 wt%) to 3.30 GJ/tCO_2 for $K_{2.5}P_{2.5}$ (K_2CO_3:PZ = 22.1:13.8 wt%). Their difference may be mainly due to the varying absorbent mass fraction ratios or lean liquid CO_2 loading. According to the Pareto set and optimal solution of the reboiler heat duty for PZ activated MDEA, it is indicated that they are considerably better than the results of 2.24 GJ/tCO2 by Zhao et al. (2017). The higher CO_2 loading of the lean liquid could be the main cause of the reduction in addition to the other operating conditions. With respect to PZ activated NH_3H_2O, the comparison suggests that the optimal compromise solution of 4.653 GJ/tCO_2 is lower than the date 5.75 GJ/tCO_2 reported by Zhang and Guo (2013a,b) but higher than the value 4.2 GJ/tCO_2 reported by Yu et al. (2011). This discrepancy may be attributed to the difference in regeneration pressure. Generally, the high operating pressure of the stripper is conducive to the reduction of the reboiler heat duty (Duan et al., 2012).

Overall, the PZ activated blended absorbents are recommended to be PZ activated MDEA when only considering the CO_2 regeneration energy consumption, followed by PZ activated K_2CO_3 and PZ activated NH_3H_2O if neglecting the effects of other operating conditions. Furthermore, to determine which is the most practical to be applied to industry, it is necessary to evaluate the benefit/cost ratio for the whole CO_2 absorption-regeneration process. Particularly, the operating costs have to be considered, including the total costs of resources (e.g., the economics of mixed absorbents) and energy consumptions and other operating costs. Meanwhile, the potential economic profit generated by the captured CO_2 is also needed for assessment, including the equivalent energy-saving benefits of carbon emission reduction and the benefits of CO_2 reuse.

4. Conclusions and perspectives

Process simulation of CO_2 capture based on the Rate-based model for typical PZ activated blended absorbents (PZ activated K_2CO_3, MDEA, and NH_3H_2O) was demonstrated to be feasible. Further modeling and optimization provide a quantitative reference for the whole post-combustion CO_2 capture system.

For the post-combustion CO_2 capture system of a 430 MW commercial power plant, the total molar concentration of the absorbent, the PZ molar concentration ratio, the lean liquid CO_2 load, the lean liquid temperature, and the rich liquid temperature were the key operating factors, while the absorbent flow rate, boiling heat duty (in the units of gigajoules per ton of CO_2) and cooling water consumption were chosen as the objective variables. According to the simulated results of PZ activated blended absorbents (PZ-K_2CO_3, PZ-MDEA, and PZ-NH_3H_2O), the multi-objective response surface models were established using 85% CO_2 capture efficiency as a constraint. On this basis, the response relationship was comprehensively examined. Finally, the optimal operations were determined for each absorbent in terms of an assessment of the optimal compromise solution.

A trade-off effect exists between the objective variables: lean molar flow rate, reboiler heat duty, and cooling water consumption. When considering the regenerative energy consumption, the absorbent for post-combustion CO_2 capture is recommended as the PZ-activated MDEA, followed by PZ-activated K_2CO_3 and PZ-activated NH_3H_2O according to the reboiler heat duty. An extensive evaluation of the benefit/cost ratio for the whole post-combustion CO_2 absorption-regeneration process is also needed to address which option is preferred and widely employed in practice.

The process methods and strategies proposed can be directly adopted to guide the comprehensive characterization, optimization, and comparison for post-combustion CO_2 capture with aqueous carbonate, amine, and ammonia. However, it should be noted that in this work only simulation of CO_2 capture by PZ-activated hybrid absorbers was performed and assessed. Further work, including alternative activated-agents and global optimization of the reactor design (including both absorber and stripper), are also needed in the future.

CRediT authorship contribution statement

Bingtao Zhao: Conceptualization, Methodology, Writing - original draft, Supervision. **Tongbo Fang:** Investigation, Data curation, Writing - original draft. **Weifeng Qian:** Investigation, Software. **Jinpeng Liu:** Investigation, Software. **Yaxin Su:** Supervision, Writing - review & editing.

Declaration of competing interest

The authors declare that they have no known competing financial interests or personal relationships that could have appeared to influence the work reported in this paper.

Acknowledgments

This work was supported by the Key Laboratory of Low-Grade Energy Utilization Technologies & Systems (Chongqing University), Ministry of Education of China, China (No. LLEUTS-202009); Natural Science Foundation of Shanghai, China (No. 17ZR1419300).

References

Afkhamipour, M., Mofarahi, M., 2018. A modeling-optimization framework for assessment of CO_2 absorption capacity by novel amine solutions: 1DMA2P, 1DEA2P, DEEA, and DEAB. J. Clean. Prod. 171, 234–249.

Ahmed, R., Liu, G., Youfaf, B., Abbas, Q., Ali, M.U., 2020. Recent advances in carbon-based renewable adsorbent for selective carbon dioxide capture and separation-A review. J. Clean. Prod. 242, 118409.

Alie, C., Backham, L., Croiset, E., Douglas, P.L., 2005. Simulation of CO_2 capture using MEA scrubbing: a flowsheet decomposition method. Energy Convers. Manag. 46 (3), 475–487.

Arshad, M., Wukovits, W., Friedl, A., 2014. Simulation of CO_2 absorption using the system K_2CO_3-Piperazine. Chemical Engineering Transactions 39 (2), 577–582.

Bishnoi, S., Rochelle, G.T., 2000. Absorption of carbon dioxide into aqueous piperazine: reaction kinetics, mass transfer and solubility. Chem. Eng. Sci. 55 (22), 5531–5543.

Bravo, J.L., Rocha, J.A., Fair, J.R., 1985. Mass transfer in gauze packings. Hydrocarb. Process. 64 (1), 91–95.

Bui, M., Gunawan, I., Verheyen, V., Feron, P., Meuleman, E., 2016. Flexible operation of CSIRO's post-combustion CO_2 capture pilot plant at the AGL Loy Yang power station. International Journal of Greenhouse Gas Control 48, 188–203.

Chapel, D., Mariz, C., Ernest, J., 1999. Recovery of CO2 from flue gases: commercial trends [R]. In: Canadian Society of Chemical Engeers Annual Meeting, Sas Katoon, Sas Katchewan, Canada, vol. 10, pp. 4–6, 1999..

Che, D., Liu, D., Zhang, Z., Wang, Y., Liu, H., 2014. Simulation and analysis of MEA absorption method for capturing CO_2 in power plants. Control Instrum. Chem. Ind. 41 (7), 797–800 [In Chinese].

Chen, Y., Kong, X., Wang, J., 2016. Aspen Plus process simulation based on different absorption system of purification of natural gas with high CO_2 content. Energy Chemical Industry 37 (5), 65–70 [In Chinese].

Chilton, T.H., Colburn, A.P., 1934. Mass Transfer (absorption) coefficients prediction from data on heat transfer and fluid friction. Ind. Eng. Chem. 26 (11), 1183–1187.

Damartzis, T., Papadopoulos, A.I., Seferlis, P., 2016. Process flowsheet design optimization for various amine-based solvents in post-combustion CO_2 capture plants. J. Clean. Prod. 111, 204–216.

Dinca, C., 2016. Critical parametric study of circulating fluidized bed combustion with CO_2 chemical absorption process using different aqueous alkanolamines. J. Clean. Prod. 112, 1136–1149.

Duan, L., Yang, Y., Zhang, S., Yang, Y., 2012. Energy consumption analysis and parameters optimization of ammonia-based CO_2 removing system from flue gas of coal fired power plant. J. North China Electr. Power Univ. (Soc. Sci.) 39 (1), 6–12 [In Chinese].

Dubois, L., Thomas, D., 2012. Screening of aqueous amine-based solvents for post-combustion CO_2 capture by chemical absorption. Chem. Eng. Technol. 35 (3), 513–524.

Dubois, L., Thomas, D., 2018. Comparison of various configurations of the absorption-regeneration process using different solvents for the post-combustion CO_2 capture applied to cement plant flue gases. International Journal of Greenhouse Gas Control 69, 20–35.

Fasihi, M., Efimova, O., Breyer, C., 2019. Techno-economic assessment of CO_2 direct air capture plants. J. Clean. Prod. 224, 957–980.

Gao, J., Chen, X., Tong, M., Kang, W., Zhou, Y., Lu, J., 2017. Experimental study of the absorption and regeneration performance of several candidate solvents for post-combustion CO_2 capture. China Pet. Process. Petrochem. Technol. 19 (4), 55–64.

Hosseinzadeh, A., Hosseinzadeh, M., Vatani, A., Mohammadi, T., 2017. Mathematical modeling for the simultaneous absorption of CO_2 and SO_2 using MEA in hollow fiber membrane contactors. Chemical Engineering & Processing Process Intensification 111, 35–45.

Huamán, R.N.E., 2017. Optimized simulation of CO_2 removal process from coal fired power plants with MEA by sensitivity analysis in aspen plus. Labor & Engenho. 11 (2), 191–207.

Izadikhah, M., 2009. Using the Hamming distance to extend TOPSIS in a fuzzy environment. J. Comput. Appl. Math. 231 (1), 200–207.

Jiang, K., Li, K., Yu, H., Chen, Z., Wardhaugh, L., Feron, P., 2017. Advancement of ammonia based post-combustion CO_2 capture using the advanced flash stripper process. Appl. Energy 202, 496–506.

Kemper, J., Ewert, G., Grünewald, M., 2011. Absorption and regeneration performance of novel reactive amine solvents for post-combustion CO_2 capture. Energy Procedia 4 (1), 232–239.

Li, B., Zhang, N., Smith, R., 2016a. Simulation and analysis of CO_2 capture process with aqueous monoethanolamine solution. Appl. Energy 161, 707–717.

Li, K., Yu, H., Feron, P., Wardhaugh, L., Tade, M., 2016b. Techno-economic assessment of stripping modifications in an ammonia-based post-combustion capture process. International Journal of Greenhouse Gas Control 53, 319–327.

Li, L., Han, W., Yu, H., Tang, H., 2013. CO_2 absorption by piperazine promoted aqueous ammonia solution: absorption kinetics and ammonia loss. Greenhouse Gases Science & Technology 3 (3), 231–245.

Liu, G., Kou, L., Li, C., 2017. Absorption Performance for CO_2 Capture Process Using MDEA-AMP Aqueous Solution, 012011.

Liu, J., Wang, S., Zhao, B., Qi, G., Chen, C., 2012. Study on mass transfer and kinetics of CO_2 absorption into aqueous ammonia and piperazine blended solutions. Chem. Eng. Sci. 75 (25), 298–308.

Luo, P., Jiao, Z., Zhang, Z., 2005. Volumetric mass transfer coefficients of dilute CO_2 absorption into mixtures of potassium carbonate and piperazine in packed column. J. Chem. Ind. Eng. 56 (1), 53–57 [In Chinese].

Molina, C.T., 2015. Assessment of different methods of CO_2 capture in post-combustion using ammonia as solvent. J. Clean. Prod. 103, 463–468.

Mores, P., Rodríguez, N., Scenna, N., Mussati, S., 2012. CO_2 capture in power plants: minimization of the investment and operating cost of the post-combustion process using MEA aqueous solution. International Journal of Greenhouse Gas Control 10 (1), 148–163.

Mudhasakul, S., Ku, H., Douglas, P.L., 2013. A simulation model of a CO_2 absorption process with methyldiethanolamine solvent and piperazine as an activator. International Journal of Greenhouse Gas Control 15 (8), 134–141.

Oexmann, J., Hensel, C., Kather, A., 2008. Post-combustion CO_2 capture from coal-fired power plants: preliminary evaluation of an integrated chemical absorption process with piperazine-promoted potassium carbonate. International Journal of Greenhouse Gas Control 2 (4), 539–552.

Oexmann, J., Kather, A., 2009. Post-combustion CO_2 capture in coal-fired power plants: comparison of integrated chemical absorption processes with piperazine promoted potassium carbonate and MEA. Energy Procedia 1 (1), 799–806.

Sakwattanapong, R., Aroonwilas, A., Veawab, A., 2005. Behavior of reboiler heat duty for CO_2 capture plants using regenerable single and blended alkanolamines. Ind. Eng. Chem. Res. 44, 4465–4473, 2005.

Samanta, A., Bandyopadhyay, S.S., 2011. Absorption of carbon dioxide into piperazine activated aqueous N-methyldiethanolamine. Chem. Eng. J. 171 (3), 734–741.

Sugeno, M., 1985. Industrial Applications of Fuzzy Control. Elsevier Science Pub. Co.

Sun, W., Shao, Y., Zhao, L., Wang, Q., 2020. Co-removal of CO_2 and particulate matter from industrial flue gas by connecting an ammonia scrubber and a granular bed filter. J. Clean. Prod. 257, 120511.

Sun, W., Yong, C., Li, M., 2005. Kinetics of the absorption of carbon dioxide into mixed aqueous solutions of 2-amino-2-methyl-l-propanol and piperazine. Chem. Eng. Sci. 60 (2), 503–516.

Wilson, M., Tontiwachwuthikul, P., Chakma, A., Idem, R., Veawab, A., Aroonwilas, A., Gelowitz, D., Stobbs, R., 2004. Evaluation of the CO_2 capture performance of the university of Regina CO_2 technology development plant and the boundary dam CO_2 demonstration plant. In: The 7th International Conference on Greenhouse Gas Control Technologies, Vancouver, Canada, Sept 5-9, 2004; peer-reviewed paper (ID No. 365).

Yeh, J.T., Resnik, K.P., Rygle, K., Pennline, H.W., 2005. Semi-batch absorption and regeneration studies for CO_2 capture by aqueous ammonia. Fuel Process. Technol. 86 (14), 1533–1546.

Yu, H., Morgan, S., Allport, A., Cottrell, A., Do, T., McGregor, J., Wardhaugh, L., Feron, P., 2011. Results from trialling aqueous NH_3-based post combustion capture in a pilot plant at munmorah power station: absorption. Chem. Eng. Res. Des. 89 (8), 1204–1215.

Yu, J., Wang, S., Yu, H., 2016. Experimental studies and rate-based simulations of CO_2, absorption with aqueous ammonia and piperazine blended solutions. International Journal of Greenhouse Gas Control 50, 135–146.

Yu, J., Wang, S., Yu, H., Wardhaugh, L., Feron, P., 2014. Rate-based modelling of CO_2 regeneration in ammonia based CO_2 capture process. International Journal of Greenhouse Gas Control 28 (2), 203–215.

Zarogiannis, T., Papadopoulos, A.I., Seferlis, P., 2016. Systematic selection of amine mixtures as post-combustion CO_2 capture solvent candidates. J. Clean. Prod. 136, 159–175.

Zhang, M., Guo, Y., 2013a. Process simulations of large-scale CO_2 capture in coal-

fired power plants using aqueous ammonia solution. International Journal of Greenhouse Gas Control 16 (10), 61–71.
Zhang, M., Guo, Y., 2013b. Rate based modeling of absorption and regeneration for CO_2 capture by aqueous ammonia solution. Appl. Energy 111 (4), 142–152.
Zhang, Y., Liu, J., Ji, Q., Luo, H., Wang, J., 2013. Process simulation and optimization of flue gas CO_2 capture by the alkanolamine solutions. Chem. Ind. Eng. Prog. 32 (4), 930–935 [In Chinese].
Zhao, B., Liu, F., Cui, Z., Liu, C., Yue, H., Tang, S., Liu, Y., Lu, H., Liang, B., 2017. Enhancing the energetic efficiency of MDEA/PZ based CO_2 capture technology for a 650 MW power plant: process improvement. Appl. Energy 185, 362–375.
Zhao, B., Su, Y., Tao, W., Li, L., Peng, Y., 2012. Post-combustion CO_2 capture by aqueous ammonia: a state-of-the-art review. International Journal of Greenhouse Gas Control 9, 355–371.
Zhou, J., Si, F., Xu, Z., 2012. Integration and Optimization of MEA Wet Decarbonization Process and 600 MW Thermal System, vol. 1. Energy Research & Utilization, pp. 44–48 [In Chinese].
Zhou, X., 2008. Simulation of CO_2 Capture System for Coal-Fired Power Plants. Chongqing University [In Chinese].